

Consequences of zero-point motion to the radial distribution function of amorphous silicon

Joseph L. Feldman, Noam Bernstein, Dimitris A. Papaconstantopoulos, Michael J. Mehl

§

Center for Computational Materials Science, Naval Research Laboratory,
Washington, D.C. 20375

Abstract.

While there have been many studies based on models of amorphous silicon, there have been surprisingly few (perhaps only one) that have seriously addressed the radial distribution function at low temperature. Our work is based in part on the so-called NRL tight binding method using parameters for silicon determined by Bernstein et al. As we have recently shown in the case of 216-atom models, upon including zero-point motion good agreement is obtained with very accurate low temperature x-ray diffraction measurements by Laaziri et al. of the radial distribution function, although, as also found by Herrero who used the Stillinger-Weber potential, a slight asymmetry of the first peak in the RDF is predicted and this asymmetry has not been observed experimentally. Upon use of an estimate of zero-point broadening from our previous work we show here that 1000-atom models lead to good agreement with experiment for the RDF. Perhaps fortuitously, we obtain models that agree with the experimentally determined second peak in the RDF for both annealed and unannealed samples: Our tight binding relaxed models based on topologies derived from the Wooten-Winer-Weaire method and the Barkema-Mousseau method yield unannealed-sample results, whereas our tight binding relaxed model based on an MD quench of the liquid using the semi-empirical interatomic potential, EDIP, of Kaxiras and coworkers yield the annealed-sample results. Finally, the significant effect of zero point motion on the first peak in the radial distribution that we obtain in the case of amorphous silicon could also have implications for other amorphous materials, e.g. SiO_2 .

1. Introduction

The natural breadth of the first peak in the radial distribution function (FPRDF) of amorphous silicon was only recently observed for the first time by Laaziri et al. [1] by carrying out X-ray diffraction measurements out to a sufficiently large Q_{\max} (maximum value of the magnitude of the diffraction vector). Their results from a polycrystal at $T = 10$ K suggest that even at this temperature the FPRDF of amorphous silicon is substantially broadened beyond the inherent static structural broadening. They obtained data for as-implanted and annealed samples and concluded that the average coordination is approximately 3.88 for the former and 3.79 for the latter. We have previously applied [2] the NRL tight-binding (TB) method to simulations of vibrational, elastic, and structural properties of two 216-atom models. We found that Laaziri *et al.*'s conclusions for the coordination might be modified if one allowed for asymmetry in the FPRDF, an asymmetry that we observed computationally both before and after applying zero-point broadening, although it is substantially more apparent in the former case. Here we present in more detail the zero-point broadening parameter computed for one of our 216-atom models, and apply it approximately to larger models. We study 1000-atom models generated by several methods: (a) the Wooten-Winer-Weaire (W) bond switching algorithm [3]; (b) quenching of the liquid state via molecular dynamics and the environment-dependent interatomic potential (EDIP) [4]; (c) an improved Wooten-Winer-Weaire method Barkema and Mousseau (BM) [5]; (d) relaxation of W, EDIP, and BM models using the conjugate gradient method with forces computed with the NRL-TB approach (the relaxed models are denoted by TB-W, TB-EDIP, and TB-BM, respectively). Compared to our original work this new analysis gives better statistics, allows us to examine the RDF at longer distances, and adds a structural model generated with another method.

2. Brief discussion of NRL tight binding

In this scheme tight binding parameters are represented by polynomial functions of interatomic distances fitted to the total energy and eigenvalues of first-principles LAPW/LDA calculations.[6] The tight binding Hamiltonian representational basis is non-orthogonal and the sum of eigenvalues of the occupied states gives the total energy. For silicon we use the sp^3 basis and included in the fit, the *crystalline* diamond-, FCC-, BCC- and SC-structure total energies (vs. volume) and electron band energies[7].

3. Brief Discussion of theory for RDF

The expression for the measured RDF is

$$J(r) = (1/N) \left\langle \sum_{i \neq j} \delta(r - r_{ij}) \right\rangle, \quad (1)$$

where the brackets denote the statistical mechanical average. To our knowledge, prior to our work only Herrero[8] calculated this quantity for an amorphous system within a quantum mechanical framework as he performed path-integral Monte-Carlo calculations for $J(r)$ with use of the Stillinger-Weber potential[9]. That procedure takes into account possible large displacements from equilibrium. However, the small displacement, harmonic approximation ought to be sufficiently accurate at low temperature. In this latter approximation,

$$J(r) = \frac{1}{N} \sum_{i \neq j} \frac{1}{\sqrt{2\pi U_{ij}^r}} \exp(-(r_{ij}^0 - r)^2 / (2U_{ij}^r)), \quad (2)$$

where

$$U_{ij}^r \equiv \langle (\hat{\mathbf{r}}_{ij} \cdot \mathbf{u}_{ij})^2 \rangle = \frac{\hbar}{8m} \sum_{\alpha} (\mathbf{e}_{ij}^{\alpha} \cdot \hat{\mathbf{r}}_{ij}^0)^2 (n + 1/2) / \omega_{\alpha} \quad (3)$$

Here r is the distance between atoms, \mathbf{u} is an atomic displacement from equilibrium, $\omega_{\alpha}(\mathbf{e}^{\alpha})$ is the α 'th normal mode eigenvalue (eigenvector), n is the phonon occupation number, and the subscripts indicate differences between atoms i and j . We shall also consider the so-called *static* structure factor obtained by replacing r_{ij} in Eq. 1 by r_{ij}^0 .

4. 216-atom model results for U_{ij}^r

In Figs. 1 we plot, as a function of r_{ij} , both U_{ij}^r and the bond stretching force constant (FC) discussed in Ref. and shown there only over the region of the FPRDF. The nature of the bond-stretching FC's appears to bifurcate at the upper end of the second peak in the RDF and this effect is present in U_{ij}^r as well. At the upper edge of the second-peak pairs of atoms of both second and third neighbor exist (note the well known absence of a peak corresponding to the third neighbor peak in the crystal). We believe these results show the distinction in character of bonding between second and third neighbor interactions. The fitted curve is given by the following expression:

$$U_{ij}^r = 0.002616 + 0.003965(r_{ij} - 2.35) + 0.00713(r_{ij} - 2.35)^2.$$

5. Results

5.1. Energetics and structural parameters

In Table 1 we give some structural parameters of interest for our TB relaxed 1000-atom models. Consistent with experiment, the density of these models at zero pressure (defined as the trace of the stress tensor[10]) are found to be less than the corresponding crystalline density, 0.05007 atoms/ \AA^3 . Upon inspecting the RDF we chose the value 2.8 \AA as the interatomic distance below which atoms are considered to be bonded. This choice, for TB-W, yields six 5-fold coordination defects, whereas, for the pristine W-model, it yields no coordination defects. In the case of TB-EDIP, there are ten 3-fold and thirty two 5-fold atoms and in the case of TB-BM there are no coordination defects. (In

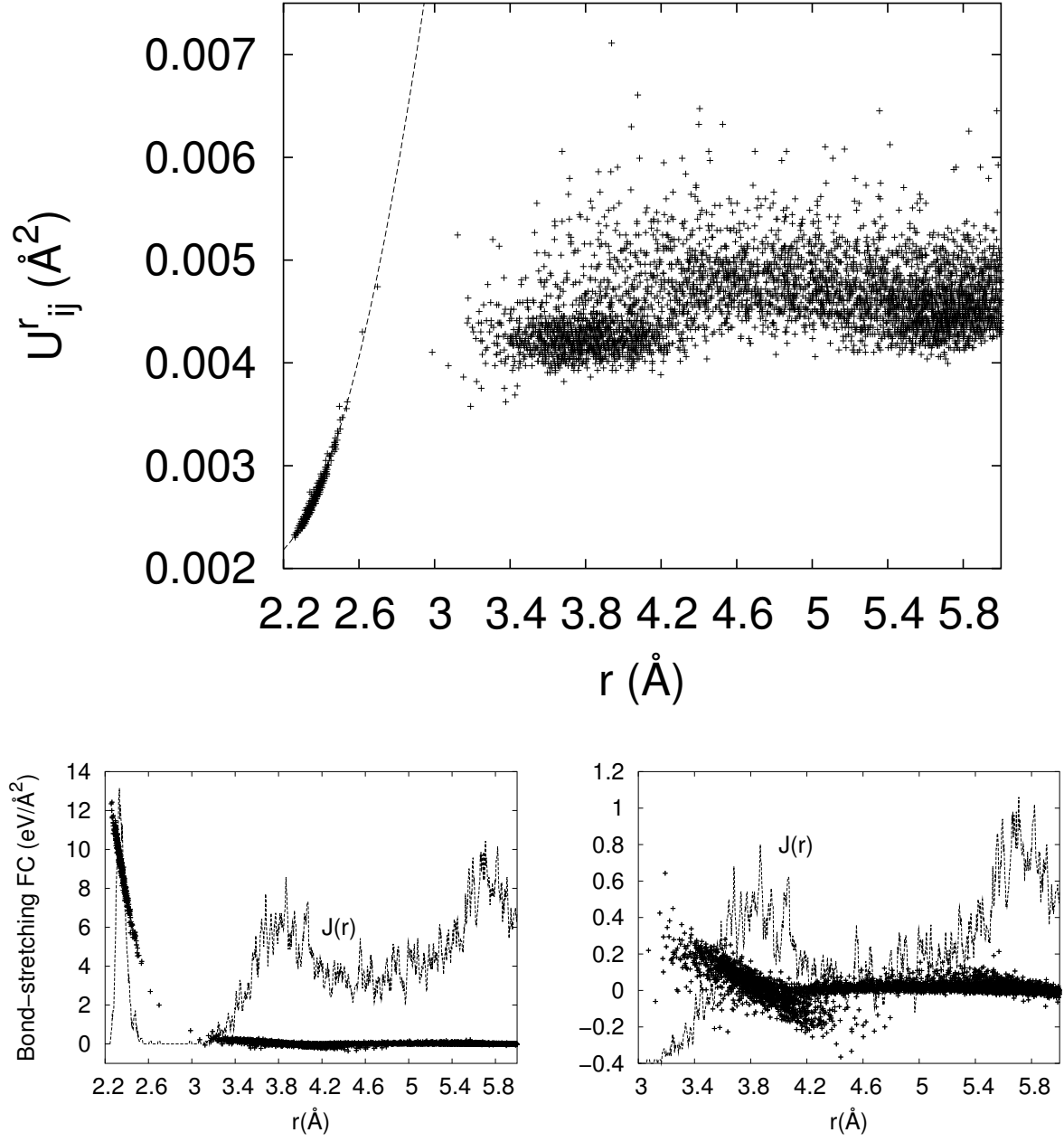


Figure 1. Comparison of zero-point broadening parameter, U_{ij}^r , bond stretching force constant and radial dependence of the RDF. The dashed line is fitted to U_{ij}^r for $r \leq 2.8$ \AA (see text). The results are based on the 216-atom TB-W model.

Table 1. Structural parameters.

Model	N_C	$(\delta V)/V_c(\%)$	N_4	θ_{ave}	$\Delta\theta_{RMS}$
TB-W	4.01	1.45	25	109.2°(108.8°)	11.0°(10.8°)
TB-EDIP	4.05	0.5	38	109.2°(108.7°)	10.5°(9.8°)
TB-BM	4.0	1.31	0	109.2°(108.7°)	10.1°(10.4°)
Exp.	≤ 3.88	≥ 1.7		.	

the table, the average coorsination is denote N_C .) Also given in the table are numbers of 4-membered rings, N_4 , in order to provide some indication of differences in topology among the models. The values of bond angles, θ , are restricted to atoms which are four-fold coordinated and the values in parentheses are results of Gaussian fits to the distribution functions for values of θ . As seen in Table 1, among our three models, TB-EDIP yields the narrowest width of the distribution of bond angle deviations, although TB-BM yields the smallest RMS bond angle deviation.

Weaire[11] and Weaire and Thorpe[12] showed, with the use of a simple tight binding model, that a band gap is obtained even if the structure lacks crystalline periodicity. Their seminal work is strictly relevant to systems with purely topological disorder. Of course, for more realistic tight-binding/structural models, even those for which all atoms are 4-fold coordinated, having a clean gap is not guaranteed due to the allowed complexity of tight binding parameters and their dependencies on interatomic distances. We give the electronic density of state information for the three models under consideration in Fig. 2. We note that our value for the gap, which is well defined only for models TB-W and TB-BM, is approximately 0.5 eV compared to the more accurate value of approximately 1 eV on the basis of *ab initio* calculations and other structural models[5, 13]. Our too-small gaps are consistent with the corresponding results for the crystal; they are due to the fact that the sp^3 set of tight binding parameters was not closely fit to the LAPW/LDA results for the conduction bands of the crystal[7]. Finally, we have obtained the following results for total energies: Relative to the total energy for the corresponding 1000-atom *crystalline* model at its equilibrium volume, we obtain increases of 0.2225, 0.2183, and 0.1958 eV/atom for TB-W, TB-EDIP, and TB-BM, respectively. These values are also in reasonable agreement with the quoted[4] experimental value of <0.19 eV/atom.

5.2. Static structural quantities

In Fig. 3 we give the FPRDF for TB-relaxed static structures. We see that there is reasonable agreement between the theoretical results for the 1000- and the previously obtained 216-atom models as well as among results for the three different methods of deriving the “pristine” models which we relaxed. The calculated FPRDF is considerably sharper and more asymmetrical than experiment, also shown in the figure.

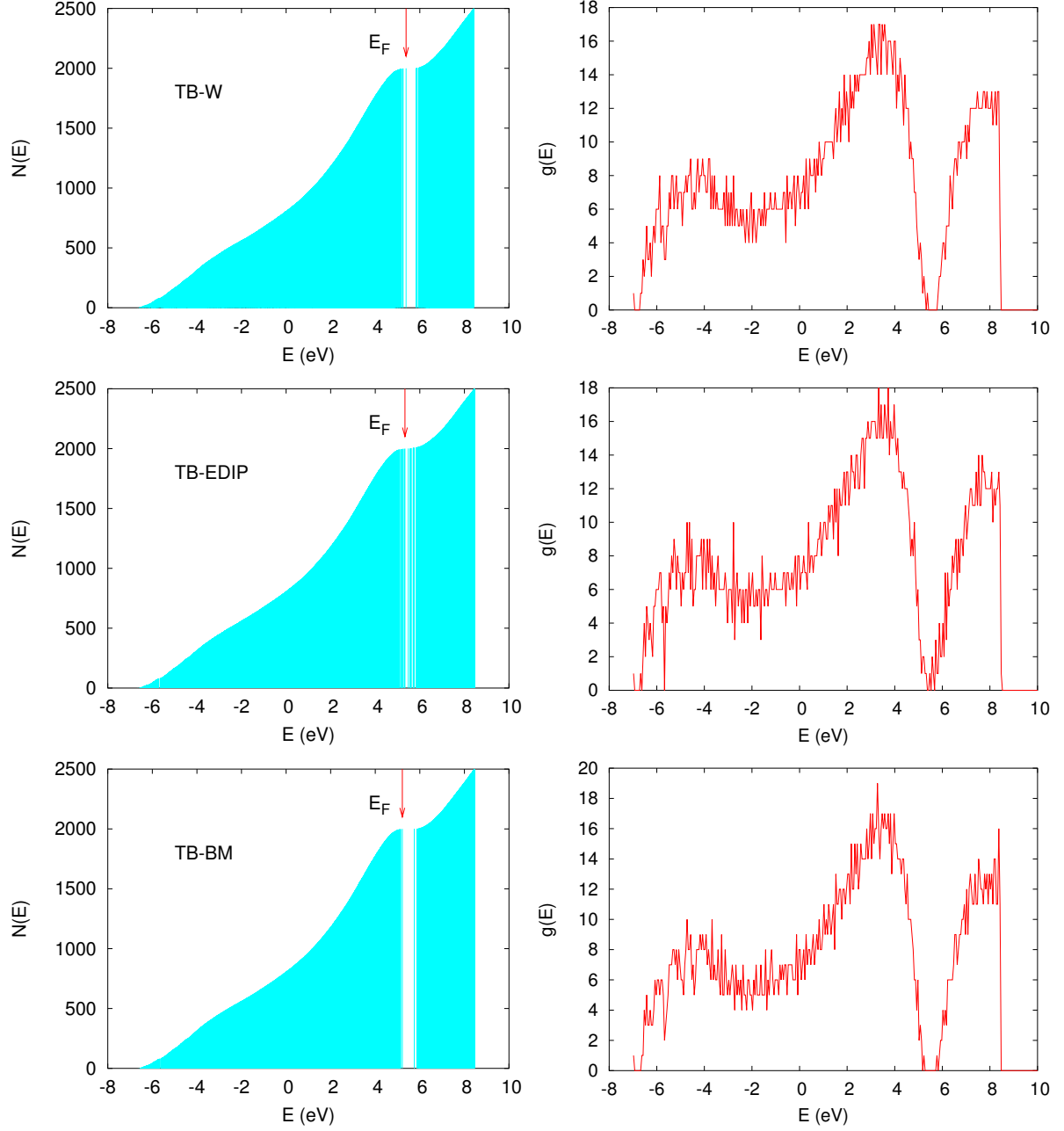


Figure 2. Electronic band states. Left hand figures give the integrated density of states and corresponding right hand figures give the density of states. The energy of the highest occupied state denoted, by E_F , and the total energy decrease in order for models TB-W, TB-EDIP and TB-BM.

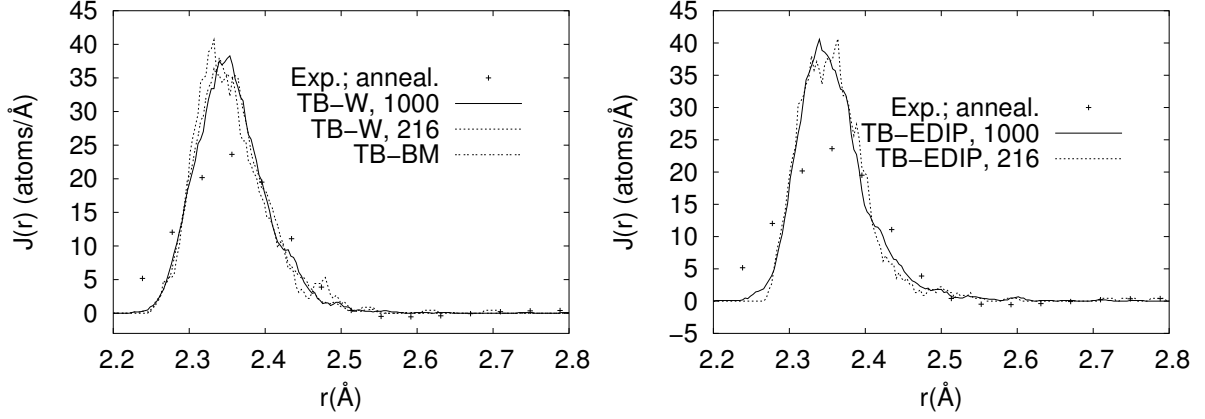


Figure 3. Static RDF's. Experimental data are included for comparison.

6. Zero-point broadened radial distribution function

For $r \leq 2.8\text{\AA}$ the broadening parameter, U_{ij}^r , was approximated by the fitted quadratic given above and for $r > 2.8\text{\AA}$, it was approximated by the constant value 0.00478\AA^2 . A test of this approximation in the case of 216-atom models yields negligible differences from the exact results. Finally in Figs. 4 and 5 we show the zero-point broadened results. There is only a small explicit zero-point effect in the region beyond the FPRDF[14], because of the already-broad features in the RDF, but the zero-point broadening in the FPRDF is large as can be seen by comparing Figs. 3 and 4.

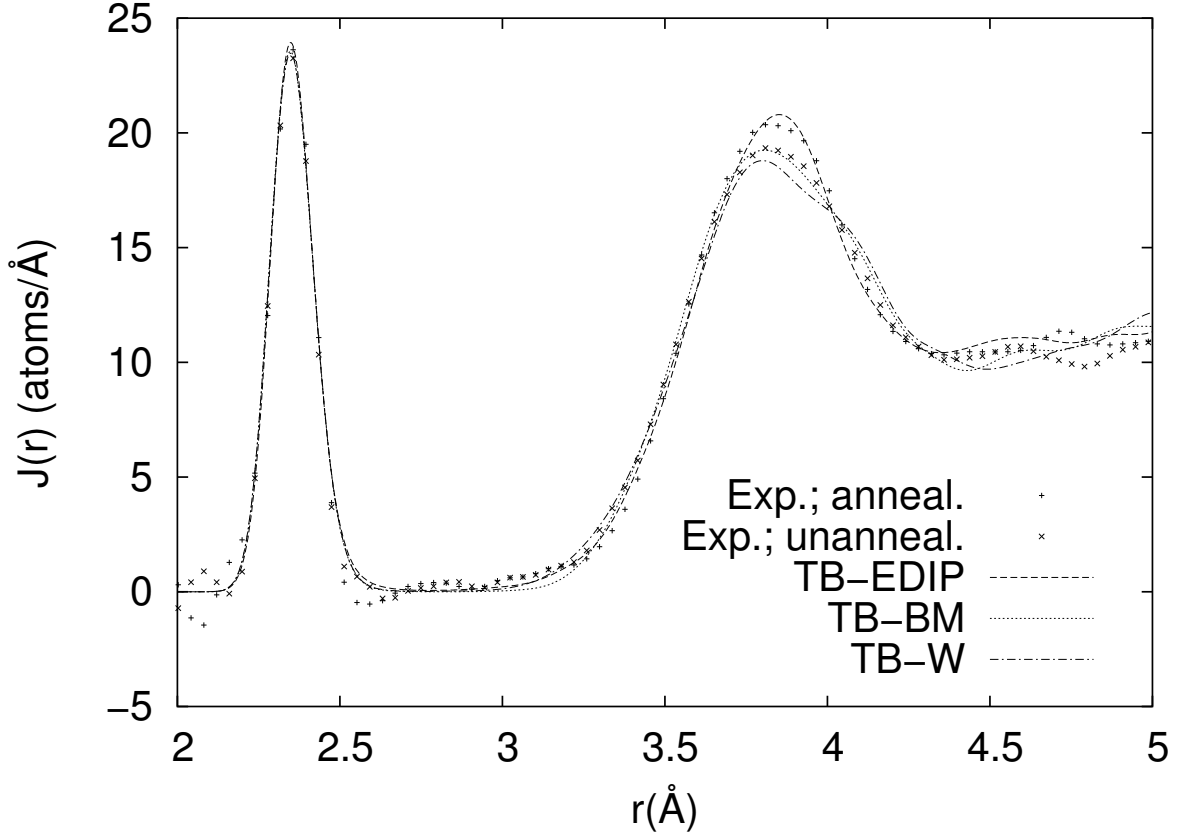


Figure 4. Comparison between theory and experiment (Ref. 1) (at $T=10\text{K}$) for first two peaks of the RDF. The theoretical quantities include the zero-point broadening (see text).

7. Conclusions

The zero-point effect in the first peak of the RDF has been shown to be important in interpreting models of amorphous silicon. As we have first discussed in another paper on 216-atom models, it has a large effect on the FPRDF within our TB approach. This result is also consistent with the interpretation of Laaziri et al. of their experimental results on both a-Si and polycrystalline Si at low temperature. By extending our method to 1000-atom models we obtain a comparison with experiment over a larger range of distances than before, and we obtain better statistical results at all distances. With regard to the overall RDF, we obtain tight binding relaxed models that agree well, if not exactly, with experiment for both as-implanted and annealed samples. However, the lowest energy model is the relaxed BM model which agrees best with experiment for the as-implanted sample. Perhaps, on the basis of NRL-TB, the topology of the EDIP model is superior to that of the BM model since EDIP yields good agreement for the annealed sample. However the coordination “defects” within the EDIP model represent a possibly serious deficiency of the model since the model yields numerous

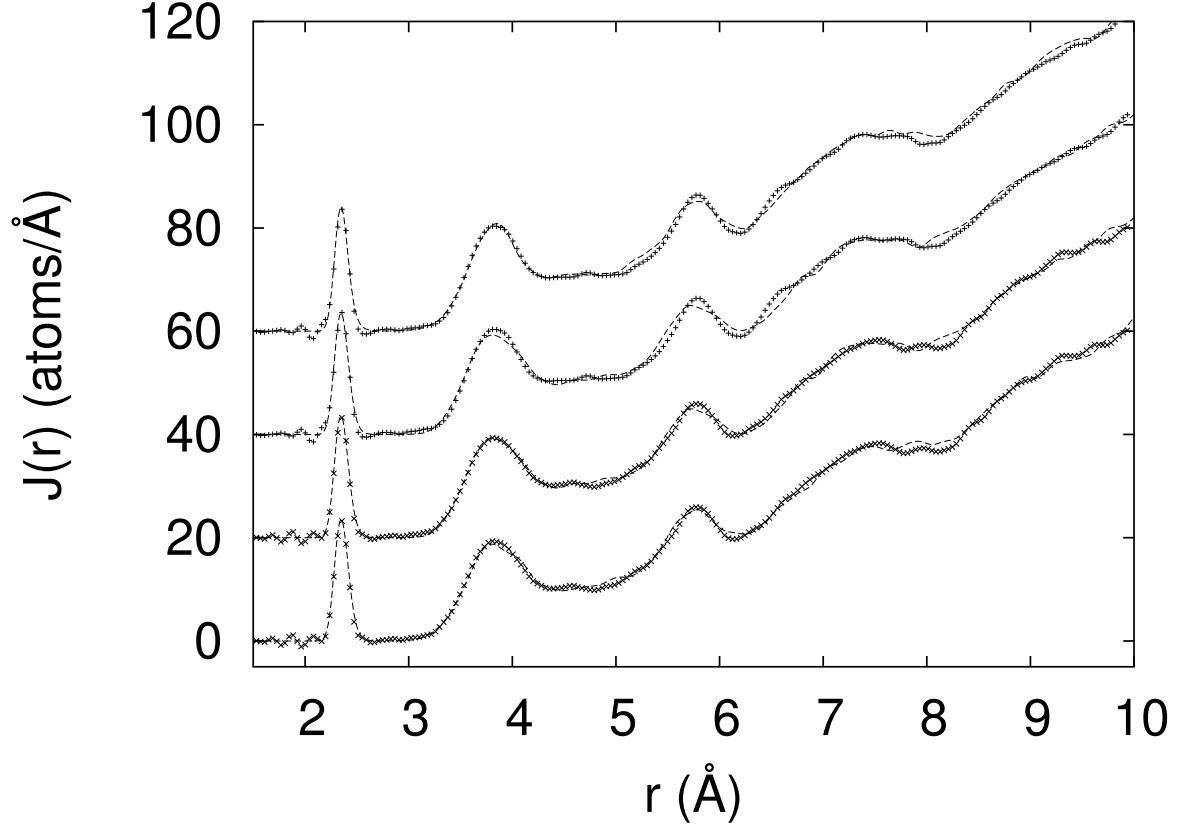


Figure 5. Comparison with experiment of zero-point broadened RDF's. The experimental data (Ref. 1) represented in the top (bottom) two curves are for the annealed (unannealed) sample. The models represented are in the order TB-EDIP, TB-BM, TB-BM, and TB-W from top to bottom.

electronic states destroying the band gap. Finally, the aforementioned results are based in part on a fitting procedure of the variance in the atomic displacements appropriate to zero-point broadening, for we have not yet obtained the full dynamical matrix for any of our 1000-atom models.

Acknowledgments

This work was supported by the U.S. Office of Naval Research. We are also grateful to Dr. S. Roorda for a helpful communication and for sending us the x-ray data of Ref. [1] for the radial distribution function.

References

- [1] Laaziri K, Kycia S, Roorda S, Chicoine M, Robertson J L, Wang J, and Moss S C 1999 *Phys Rev Lett* **82** 3460
Laaziri K, Kycia S, Roorda S, Chicoine M, Robertson J L, Wang J and Moss S C 1999 *Phys Rev B* **60** 13520
- [2] Feldman J L, Bernstein N, Papaconstantopoulos D A and Mehl M J 2004 *Phys Rev B* accepted for publication
Feldman J L, Bernstein N, Papaconstantopoulos D A and Mehl M J 2004 *Preprint cond-mat/0405327* unpublished
- [3] Wooten F, Winer K and Weaire D 1985 *Phys Rev Lett* **54** 1392
Feldman J L, Kluge M D, Allen P B and Wooten F 1993 *Phys Rev B* **48** 12589
- [4] Keblinski P, Bazant M Z, Dash R K and Treacy M M 2002 *Phys Rev B* **66** 064104
- [5] Barkema G T and Mousseau N 2000 *Phys Rev B* **62** 4985
- [6] Cohen R E, Mehl M J and Papaconstantopoulos D A 1994 *Phys Rev B* **50** 14694
Mehl M J and Papaconstantopoulos D A 1996 *Phys Rev B* **54** 4519
- [7] Bernstein N, Mehl M J, Papaconstantopoulos D A, Papanicolaou N I, Bazant M Z and Kaxiras E 2000 *Phys Rev B* **62** 4477
Bernstein N, Mehl M J, Papaconstantopoulos D A, Papanicolaou N I, Bazant M Z and Kaxiras E 2002 *Phys Rev B* **65** 249902 (E)
- [8] Herrero C P 1998 *Europhys. Lett.* **44** 734
- [9] Stillinger F H and Weber T A 1985 *Phys Rev B* **31** 5262
- [10] Stress tensor components of about 0.8 GPa or less are obtained due to the finite size of the models and cubic boundary conditions
- [11] Weaire D 1971 *Phys. Rev. Lett.* **26** 1541
- [12] Weaire D and Thorpe M F 1971 *Phys Rev B* **4** 2508
- [13] Nakhmanson S M, Mousseau N, Barkema G T, Voyles P M and Drabold D A 2001 *International Journal of Modern Physics B* **15** 3253
- [14] Effectively, the zero-point broadening of the second peak in the RDF was discussed, on the basis of x-ray diffraction data on polycrystalline silicon, in the second reference of Ref. 1